Reduction of the Ring Size of Radiolabeled Lactam Bridge–Cyclized α-MSH Peptide, Resulting in Enhanced Melanoma Uptake

Haixun Guo[1], Jianquan Yang[1], Fabio Gallazzi[2], and Yubin Miao[1,3,4]

[1]College of Pharmacy, University of New Mexico, Albuquerque, New Mexico; [2]Department of Biochemistry, University of Missouri, Columbia, Missouri; [3]Cancer Research and Treatment Center, University of New Mexico, Albuquerque, New Mexico; and [4]Department of Dermatology, University of New Mexico, Albuquerque, New Mexico

The purpose of this study was to examine the profound effect of the ring size of the radiolabeled lactam bridge–cyclized α-melanocyte–stimulating hormone (α-MSH) peptide on its melanoma-targeting properties. **Methods:** A novel cyclic α-MSH peptide, 1,4,7,10-tetraazacyclododecane-1,4,7,10-tetraacetic acid-Nle-c[Asp-His-D-Phe-Arg-Trp-Lys]-CONH$_2$ (DOTA-Nle-CycMSH$_{hex}$), was synthesized and radiolabeled with ^{111}In. The melanocortin-1 receptor–binding affinity of DOTA-Nle-CycMSH$_{hex}$ was determined in B16/F1 melanoma cells. The internalization and efflux of ^{111}In-DOTA-Nle-CycMSH$_{hex}$ were examined in B16/F1 cells. The melanoma-targeting properties and SPECT/CT characteristics of ^{111}In-DOTA-Nle-CycMSH$_{hex}$ were determined in B16/F1 melanoma–bearing C57 mice. **Results:** DOTA-Nle-CycMSH$_{hex}$ displayed 1.77 nM receptor-binding affinity. ^{111}In-DOTA-Nle-CycMSH$_{hex}$ exhibited rapid internalization and extended retention in B16/F1 cells. The tumor uptake of ^{111}In-DOTA-Nle-CycMSH$_{hex}$ was 24.94% ± 4.58% and 10.53% ± 1.11% injected dose per gram at 0.5 and 24 h after injection, respectively. Greater than 82% of the injected radioactivity was cleared through the urinary system by 2 h after injection. The tumor-to-kidney uptake ratios reached 2.04 and 1.70 at 2 and 4 h after injection, respectively. Flank melanoma tumors were clearly visualized by SPECT/CT using ^{111}In-DOTA-Nle-CycMSH$_{hex}$ as an imaging probe at 2 and 24 h after injection. The radioactivity accumulation in normal organs, except for the kidneys, was low at 2, 4, and 24 h after injection. **Conclusion:** The reduction of the peptide ring size dramatically increased the melanoma uptake and decreased the renal uptake of ^{111}In-DOTA-Nle-CycMSH$_{hex}$, providing a new insight into the design of a novel radiolabeled lactam bridge–cyclized α-MSH peptide for melanoma imaging and treatment.

Key Words: melanoma imaging; radiolabeled cyclic peptide; α-melanocyte–stimulating hormone; small-animal imaging

Skin cancer is the most commonly diagnosed cancer in the United States. Melanoma accounts for less than 5% of skin cancer cases but causes greater than 75% of deaths from skin cancer. It is predicted that 68,720 new cases will be diagnosed and 8,650 deaths will occur in 2009 (*1*). Early diagnosis and prompt surgical removal are the best opportunities for a patient's cure, because no curative treatment exists for metastatic melanoma. Despite the clinical use of ^{18}F-FDG for PET diagnosis and staging of melanoma, ^{18}F-FDG is not a melanoma-specific imaging agent and is also not effective in imaging small melanoma metastases (<5 mm) and melanomas that have primary energy sources other than glucose (*2–4*). Alternatively, melanocortin-1 (MC1) receptor is a distinct molecular target because of its overexpression on both human and mouse melanoma cells (*5–9*). Radiolabeled α-melanocyte–stimulating hormone (α-MSH) peptides can bind the MC1 receptors with nanomolar binding affinities (*10–20*) and represent a class of promising melanoma-specific radiopharmaceuticals for melanoma imaging and therapy.

Recently, we have developed a novel class of ^{111}In-labeled lactam bridge–cyclized 1,4,7,10-tetraazacyclododecane-1,4,7,10-tetraacetic acid (DOTA)-conjugated α-MSH peptides for melanoma detection (*21,22*). Lactam bridge cyclization was used to improve the stabilities of the α-MSH peptides against the proteolytic degradations in vivo and enhance the binding affinities of the α-MSH peptides through stabilization of their secondary structures such as β-turns (*23–26*). The radiometal chelator DOTA was attached to the N terminus of the lactam bridge–cyclized α-MSH peptide (12 amino acids in the peptide ring) for ^{111}In radiolabeling. For instance, ^{111}In-DOTA-GlyGlu-CycMSH (^{111}In-DOTA-Gly-Glu-c[Lys-Nle-Glu-His-D-Phe-Arg-Trp-Gly-Arg-Pro-Val-Asp]) exhibited high MC1 receptor–mediated tumor uptake (10.40 ± 1.40 percentage injected dose per gram [%ID/g] at 2 h after injection) in flank B16/F1 melanoma–bearing C57 mice (*21*). Both primary and pulmonary metastatic melanoma flank lesions were clearly visualized by small-animal SPECT/CT using

^{111}In-DOTA-GlyGlu-CycMSH as an imaging probe (21,22), highlighting its potential as an effective imaging probe for melanoma detection.

One advantage of the lactam bridge–cyclized α-MSH peptide is that the peptide ring size can be finely modified by either adding or deleting amino acids without sacrificing the binding affinity of the peptide (21,22). The studies on the α-MSH peptide agonists for the MC1 receptor revealed that the lactam bridge–cyclized α-MSH peptide with a 6-amino acid peptide ring (Ac-Nle-c[Asp-His-D-Phe-Arg-Trp-Lys(CONH$_2$)]) displayed not only higher MC1 receptor–binding affinity but also a slower MC1 receptor dissociation rate than the native α-MSH peptide (Ac-Ser-Tyr-Ser-Met-Glu-His-Phe-Arg-Trp-Gly-Lys-Pro-Val-NH$_2$) (27,28). A slow MC1 receptor dissociation rate might contribute to the prolonged biologic activity of Ac-Nle-c[Asp-His-D-Phe-Arg-Trp-Lys(CONH$_2$) in vitro and in vivo (27). In this study, we conjugated the radiometal chelator DOTA to the N terminus of the Ac-Nle-c[Asp-His-D-Phe-Arg-Trp-Lys(CONH$_2$) peptide to generate a novel DOTA-conjugated lactam bridge–cyclized α-MSH peptide with a 6-amino acid peptide ring (DOTA-Nle-CycMSH$_{hex}$) to examine the effect of peptide ring size on its melanoma-targeting and pharmacokinetic properties. The MC1 receptor–binding affinity of DOTA-Nle-CycMSH$_{hex}$ was determined in B16/F1 melanoma cells. DOTA-Nle-CycMSH$_{hex}$ was radiolabeled with ^{111}In, a commercially available diagnostic radionuclide with a half-life of 2.8 d. The melanoma-targeting and pharmacokinetic properties and SPECT/CT of ^{111}In-labeled DOTA-Nle-CycMSH$_{hex}$ were determined in B16/F1 melanoma–bearing C57 mice.

MATERIALS AND METHODS

Chemicals and Reagents

Amino acid and resin were purchased from Advanced Chem-Tech Inc. and Novabiochem. DOTA-tri-t-butyl ester was purchased from Macrocyclics Inc. [111]InCl$_3$ was purchased from Trace Life Sciences, Inc. ^{125}I-Tyr^2-[Nle^4, D-Phe^7]-α-MSH ([125]I-(Tyr^2)-NDP-MSH) was obtained from PerkinElmer, Inc. All other chemicals used in this study were purchased from Thermo Fischer Scientific and used without further purification. B16/F1 melanoma cells were obtained from American Type Culture Collection.

Peptide Synthesis

DOTA-Nle-CycMSH$_{hex}$ was synthesized using standard fluorenylmethyloxycarbonyl chemistry. Briefly, an intermediate scaffold of (tBu)$_3$DOTA-Nle-Asp(O-2-PhiPr)-His(Trt)-D-Phe-Arg(Pbf)-Trp(Boc)-Lys(Dde) was synthesized on H$_2$N-Sieber amide resin by an Advanced ChemTech multiple-peptide synthesizer. The protecting group of Dde was removed by 2% hydrazine for peptide cyclization. The protecting group of 2-phenylisopropyl from the Asp residue was removed, and the protected peptide was cleaved from the resin by treatment with a mixture of 2.5% of trifluoroacetic acid (TFA) and 5% of triisopropylsilane for 1 h. After precipitation with ice-cold ether and characterization by liquid chromatography–mass spectroscopy (LC-MS), the protected peptide was dissolved in H$_2$O:CH$_3$CN (30:70) and lyophilized to remove the reagents such as TFA and triisopropylsilane. The protected peptide was further

cyclized by coupling the carboxylic group from the Asp with the ε-amino group from the Lys. The cyclization reaction was achieved by an overnight reaction in dimethylformamide using benzotriazole-1-yl-oxy-tris-pyrrolidino-phosphonium-hexafluorophosphate as a coupling agent in the presence of N,N-diisopropylethylamine. After characterization by LC-MS, the cyclized protected peptide was dissolved in H$_2$O:CH$_3$CN (30:70) and lyophilized to remove the reagents such as benzotriazole-1-yl-oxy-tris-pyrrolidino-phosphonium-hexafluorophosphate and N,N-diisopropylethylamine. The protecting groups were totally removed by treatment with a mixture of TFA, thioanisole, phenol, water, ethanedithiol, and triisopropyl-silane (87.5:2.5:2.5:2.5:2.5:2.5) for 4 h at room temperature (25°C). The peptide was precipitated and washed with ice-cold ether 4 times, purified by reversed-phase (RP) high-performance liquid chromatography (HPLC), and characterized by LC-MS.

In Vitro Competitive Binding Assay

The inhibitory concentration of 50% (IC$_{50}$) value of DOTA-Nle-CycMSH$_{hex}$ was determined by an in vitro competitive binding assay according to our previously published procedure (21). B16/F1 cells were harvested and seeded into a 24-well cell culture plate (5×10^5 cells per well) and incubated at 37°C overnight. After the cells were washed twice with binding medium, Dulbecco's modified Eagle's medium with 25 mM N-(2-hydroxyethyl)-piperazine-N′-(2-ethanesulfonic acid) (pH 7.4, 0.2% bovine serum albumin [BSA], and 0.3 mM 1,10-phenathroline), they were incubated at room temperature (25°C) for 2 h with approximately 60,000 counts per minute of ^{125}I-Tyr^2-NDP-MSH in the presence of increasing concentrations (10^{-12} to 10^{-5} M) of DOTA-Nle-CycMSH$_{hex}$ in 0.3 mL of binding medium. The reaction medium was aspirated after the incubation. The cells were rinsed twice with 0.5 mL of ice-cold, pH 7.4, 0.2% BSA/0.01 M phosphate-buffered saline and lysed in 0.5 mL of 1N NaOH for 5 min. The activities associated with cells were measured in a Wallac 1480 automated γ-counter (PerkinElmer). The IC$_{50}$ value of the peptide was calculated using Prism software (GraphPad Software).

Peptide Radiolabeling with [111]In

^{111}In-DOTA-Nle-CycMSH$_{hex}$ was prepared in a 0.5 M NH$_4$OAc-buffered solution at pH 4.5 according to our published procedure (21). Briefly, 50 μL of [111]InCl$_3$ (37–74 MBq [1–2 mCi] in 0.05 M HCl aqueous solution), 10 μL of a 1 mg/mL aqueous solution of DOTA-Nle-CycMSH$_{hex}$, and 400 μL of 0.5 M NH$_4$OAc (pH 4.5) were added into a reaction vial and incubated at 75°C for 45 min. After the incubation, 10 μL of 0.5% ethylenediaminetetraacetic acid aqueous solution were added into the reaction vial to scavenge potential unbound [111]In^{3+} ions. The radiolabeled peptide was purified to a single species by Waters RP HPLC on a Grace Vydac C-18 reversed-phase analytic column using a 20-min gradient of 18%−28% acetonitrile in 20 mM HCl aqueous solution with a flow rate of 1.0 mL/min. The purified peptide sample was purged with N$_2$ gas for 20 min to remove the acetonitrile. The pH of the final solution was adjusted to 7.4 with 0.1N NaOH and sterile normal saline for animal studies. The in vitro serum stability of HPLC-purified ^{111}In-DOTA-Nle-CycMSH$_{hex}$ was determined by incubation in mouse serum at 37°C for 24 h and monitored for degradation by RP HPLC.

Cellular Internalization and Efflux of ^{111}In-DOTA-Nle-CycMSH$_{hex}$

Cellular internalization and efflux of ^{111}In-DOTA-Nle-CycMSH$_{hex}$ were evaluated in B16/F1 melanoma cells. After being

washed twice with the binding medium, the B16/F1 cells seeded in cell culture plates were incubated at 25°C for 20, 40, 60, 90, and 120 min ($n = 3$) in the presence of approximately 200,000 counts per minute of HPLC-purified ^{111}In-DOTA-Nle-CycMSH$_{hex}$. After incubation, the reaction medium was aspirated, and the cells were rinsed with 2×0.5 mL of ice-cold, pH 7.4, 0.2% BSA/0.01 M phosphate-buffered saline. Cellular internalization of ^{111}In-DOTA-Nle-CycMSH$_{hex}$ was assessed by washing the cells with acidic buffer (40 mM sodium acetate [pH 4.5] containing 0.9% NaCl and 0.2% BSA) to remove the membrane-bound radioactivity. The remaining internalized radioactivity was obtained by lysing the cells with 0.5 mL of 1N NaOH for 5 min. Membrane-bound and internalized ^{111}In activities were counted in a γ-counter. Cellular efflux of ^{111}In-DOTA-Nle-CycMSH$_{hex}$ was determined by incubating the B16/F1 cells with ^{111}In-DOTA-Nle-CycMSH$_{hex}$ for 2 h at 25°C, removing nonspecifically bound activity with 2×0.5 mL of ice-cold phosphate-buffered saline rinse, and monitoring radioactivity released into the cell culture medium. At 20, 40, 60, 90, and 120 min, the radioactivities on the cell surface and inside the cells were separately collected and counted in a γ-counter.

Biodistribution Studies

All the animal studies were conducted in compliance with Institutional Animal Care and Use Committee approval. The mice were housed 5 animals per cage in sterile microisolator cages in a temperature- and humidity-controlled room with a 12-h light/12-h dark schedule. The pharmacokinetics of ^{111}In-DOTA-Nle-CycMSH$_{hex}$ were determined in B16/F1 melanoma–bearing C57 female mice (Harlan). C57 mice were subcutaneously inoculated on the right flank with 1×10^6 B16/F1 cells. The weight of tumors reached approximately 0.2 g 10 d after cell inoculation. Each melanoma-bearing mouse was injected with 0.037 MBq (1 μCi) of ^{111}In-DOTA-Nle-CycMSH$_{hex}$ via the tail vein. Groups of 5 mice were sacrificed at 0.5, 2, 4, and 24 h after injection, and tumors and organs of interest were harvested, weighed, and counted. Blood values were taken as 6.5% of the whole-body weight. The tumor uptake specificity of ^{111}In-DOTA-Nle-CycMSH$_{hex}$ was determined by coinjecting 10 μg of unlabeled NDP-MSH, a linear α-MSH peptide analog with picomolar affinity for the MC1 receptor present on the melanoma cells. To examine whether L-lysine coinjection can reduce the renal uptake, a group of 5 mice was injected with a mixture of 12 mg of L-lysine and 0.037 MBq (1 μCi) of ^{111}In-DOTA-Nle-CycMSH$_{hex}$. The mice were sacrificed at 2 h after injection. The tumor and organs of interest were harvested, weighed, and counted.

Melanoma Imaging with ^{111}In-DOTA-Nle-CycMSH$_{hex}$

Two B16/F1 melanoma–bearing C57 mice (10 d after the cell inoculation) were injected with 37 MBq (1 mCi) of ^{111}In-DOTA-Nle-CycMSH$_{hex}$ via the tail vein. The mice were sacrificed for small-animal SPECT/CT (Nano-SPECT/CT; Bioscan) at 2 and 24 h after injection. The 9-min CT scan was immediately followed by the whole-body SPECT scan. The SPECT scans of 24 projections were acquired, and total acquisition time was approximately 60 min. Reconstructed data from SPECT and CT were visualized and coregistered using InVivoScope (Bioscan).

Urinary Metabolites of ^{111}In-DOTA-Nle-CycMSH$_{hex}$

The mouse used for the imaging study (2 h after injection) was euthanized, and the urine was collected for identification of the metabolites. The urinary sample was centrifuged at 16,000g for 5 min before the HPLC analysis. The radioactive metabolite in the urine was analyzed by injecting aliquots of urine into the chomatograph. A 20-min gradient of 18%−28% acetonitrile/20 mM HCl was used for the urine analysis.

Statistical Analysis

Statistical analysis was performed using the Student t test for unpaired data. A 95% confidence level was chosen to determine the significance between the tumor uptake of ^{111}In-DOTA-Nle-CycMSH$_{hex}$ with or without NDP-MSH coinjection and the renal uptake of ^{111}In-DOTA-Nle-CycMSH$_{hex}$ with or without L-lysine coinjection in the biodistribution studies described earlier. Differences at the 95% confidence level ($P < 0.05$) were considered significant.

RESULTS

To examine the profound effect of peptide ring size on melanoma and kidney uptake of the ^{111}In-labeled lactam bridge–cyclized α-MSH peptide, a novel peptide of DOTA-Nle-CycMSH$_{hex}$ was synthesized and purified by RP HPLC. The identity of the peptide was confirmed by electrospray ionization mass spectrometry (molecular weight, 1,368.5; calculated molecular weight, 1,368.2). DOTA-Nle-CycMSH$_{hex}$ displayed greater than 95% purity, with 30% overall synthetic yield. The schematic structures of DOTA-Nle-CycMSH$_{hex}$ and DOTA-GlyGlu-CycMSH are shown in Figure 1. Figure 2 illustrates the synthetic scheme of DOTA-Nle-CycMSH$_{hex}$. The competitive binding curve of DOTA-Nle-CycMSH$_{hex}$ is presented in Figure 3A. The IC$_{50}$ value of DOTA-Nle-CycMSH$_{hex}$ was 1.77 nM in B16/F1 cells.

The peptide was readily labeled with ^{111}In in 0.5 M ammonium acetate at pH 4.5 with greater than 95% radiolabeling yield. ^{111}In-DOTA-Nle-CycMSH$_{hex}$ was completely separated from its excess nonlabeled peptide by RP HPLC. The retention time of ^{111}In-DOTA-Nle-CycMSH$_{hex}$ was 10.7 min. ^{111}In-DOTA-Nle-CycMSH$_{hex}$ showed greater than 98% radiochemical purity after the HPLC purification. ^{111}In-DOTA-Nle-CycMSH$_{hex}$ was stable in mouse serum at 37°C for 24 h. Only the ^{111}In-DOTA-Nle-CycMSH$_{hex}$ was detected by RP HPLC after 24 h of incubation.

Cellular internalization and efflux of ^{111}In-DOTA-Nle-CycMSH$_{hex}$ were evaluated in B16/F1 cells. Figures 3B and 3C illustrate the cellular internalization and efflux of ^{111}In-DOTA-Nle-CycMSH$_{hex}$, respectively. ^{111}In-DOTA-Nle-CycMSH$_{hex}$ exhibited rapid cellular internalization and extended cellular retention. At 20 and 120 min after incubation, 72.9% ± 3.5% and 88.3% ± 0.7%, respectively, of the cellular uptake of ^{111}In-DOTA-Nle-CycMSH$_{hex}$ activity had internalized in the B16/F1 cells. Cellular efflux results demonstrated that 89.5% ± 1.9% of internalized ^{111}In-DOTA-Nle-CycMSH$_{hex}$ activity remained inside the cells 2 h after the cells were incubated in culture medium.

The melanoma-targeting and pharmacokinetic properties of ^{111}In-DOTA-Nle-CycMSH$_{hex}$ were determined in B16/F1 melanoma–bearing C57 mice. The biodistribution results of ^{111}In-DOTA-Nle-CycMSH$_{hex}$ are shown in Table 1.
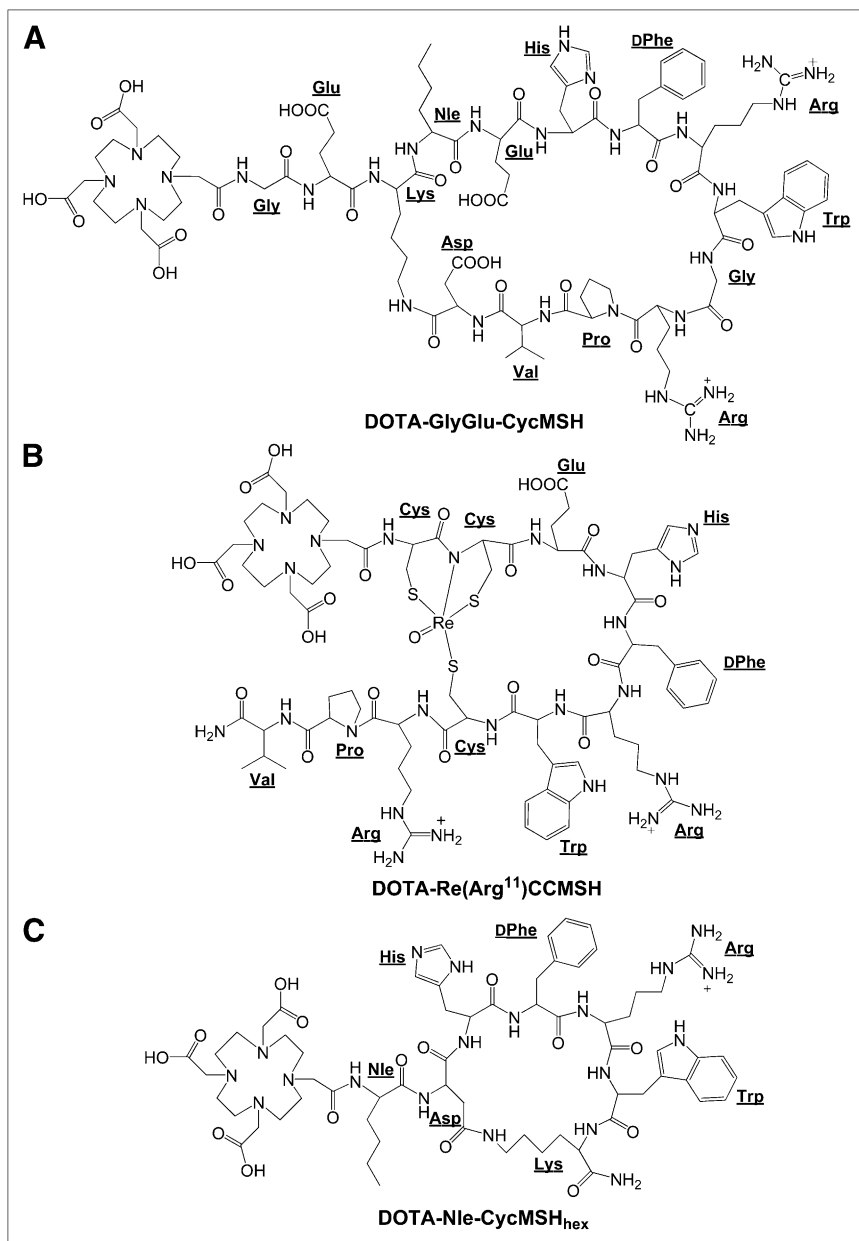
FIGURE 1. Structures of DOTA-GlyGlu-CycMSH (A), DOTA-Re(Arg[11])CCMSH (B), and DOTA-Nle-CycMSH_hex (C).

^{111}In-DOTA-Nle-CycMSH_hex exhibited rapid high melanoma uptake and prolonged tumor retention in melanoma-bearing mice. At 0.5 h after injection, ^{111}In-DOTA-Nle-CycMSH_hex reached its peak tumor uptake of 24.94 ± 4.58 %ID/g. At 4 and 24 h after injection, 17.01 ± 2.54 %ID/g and 10.53 ± 1.11 %ID/g of the ^{111}In-DOTA-Nle-CycMSH_hex activity, respectively, remained in the tumors. In the melanoma uptake blocking study, the tumor uptake of ^{111}In-DOTA-Nle-CycMSH_hex with 10 μg of nonradiolabeled NDP-MSH coinjection was only 4.2% of the tumor uptake without NDP-MSH coinjection at 2 h after dose administration ($P <$ 0.05), demonstrating that the tumor uptake was specific and MC1 receptor–mediated. Whole-body clearance of ^{111}In-DOTA-Nle-CycMSH_hex was rapid, with approximately 82% of the injected radioactivity cleared through the urinary system by 2 h after injection (Table 1). Normal-organ uptake of ^{111}In-DOTA-Nle-CycMSH_hex was low (<1.89 %ID/g), except for the kidneys, at 2, 4, and 24 h after injection. High tumor-to-blood and high tumor–to–normal-organ uptake ratios were achieved as early as 0.5 h after injection (Table 1). As the major excretion pathway of ^{111}In-DOTA-Nle-CycMSH_hex, the kidney uptake was 16.20 ± 4.32 %ID/g at 0.5 h after injection and decreased to 9.31 ± 0.91 %ID/g at 24 h after injection. The tumor-to-kidney uptake ratios of ^{111}In-DOTA-Nle-CycMSH_hex are presented in Figure 4. The tumor-to-kidney uptake ratios of ^{111}In-DOTA-Nle-CycMSH_hex were 2.04, 1.70, and 1.13 at 2, 4, and 24 h, respectively, after injection. Coinjection of NDP-MSH did not reduce renal uptake of ^{111}In-DOTA-Nle-CycMSH_hex activity at 2 h after injection, indicating that renal uptake
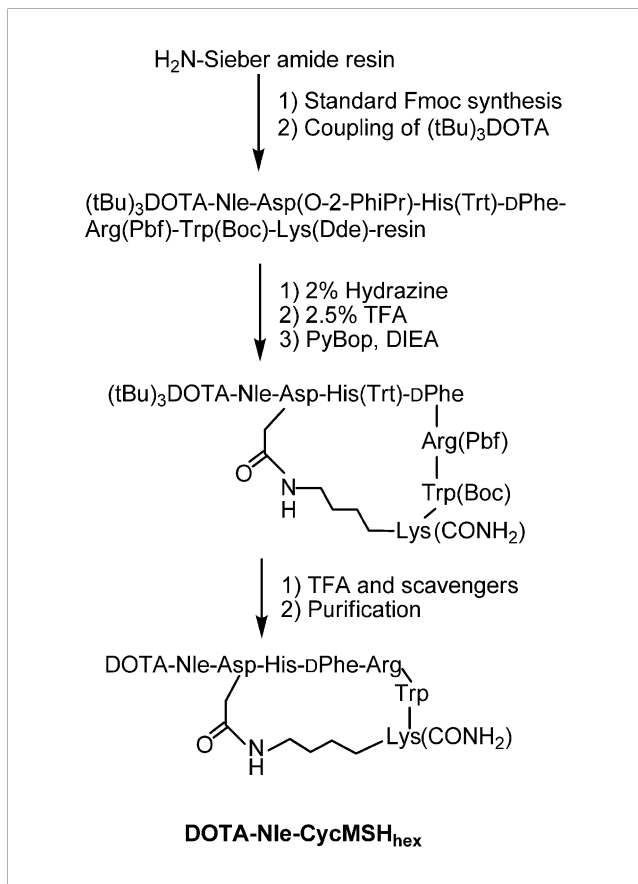
FIGURE 2. Synthetic scheme of DOTA-Nle-CycMSH$_{hex}$.

FIGURE 3. Competitive binding curve (A) of DOTA-Nle-CycMSH$_{hex}$ in B16/F1 melanoma cells. IC$_{50}$ value of DOTA-Nle-CycMSH$_{hex}$ was 1.77 nM. Cellular internalization (B) and efflux (C) of ^{111}In-DOTA-Nle-CycMSH$_{hex}$ in B16/F1 melanoma cells at 25°C. Total bound radioactivity (♦), internalized activity (■), and cell membrane activity (▲) were presented as counts per minute (cpm).

was not MC1 receptor–mediated. Coinjection of L-lysine significantly ($P < 0.05$) reduced kidney uptake by 30% at 2 h after injection (Table 1).

Two B16/F1 melanoma–bearing C57 mice were separately injected with 37 MBq (1 mCi) of ^{111}In-DOTA-Nle-CycMSH$_{hex}$ through the tail vein to visualize the tumors at 2 and 24 h after dose administration. The whole-body SPECT/CT images are presented in Figures 5A and 5B. Flank melanoma tumors were clearly visualized by SPECT/CT at 2 and 24 h after injection of ^{111}In-DOTA-Nle-CycMSH$_{hex}$. In agreement with the biodistribution results, both images showed high tumor–to–normal-organ uptake ratios except for the kidneys. The urinary metabolite of ^{111}In-DOTA-Nle-CycMSH$_{hex}$ was analyzed by RP HPLC at 2 h after injection. Figure 5C illustrates the urinary HPLC profile of ^{111}In-DOTA-Nle-CycMSH$_{hex}$. ^{111}In-DOTA-Nle-CycMSH$_{hex}$ remained intact in the urine 2 h after injection.

DISCUSSION

Cyclization strategies using a disulfide bridge, a lactam bridge, and metal coordination have been successfully applied to cyclize the α-MSH peptides to enhance the binding affinities and in vivo stabilities of the peptides (23–26).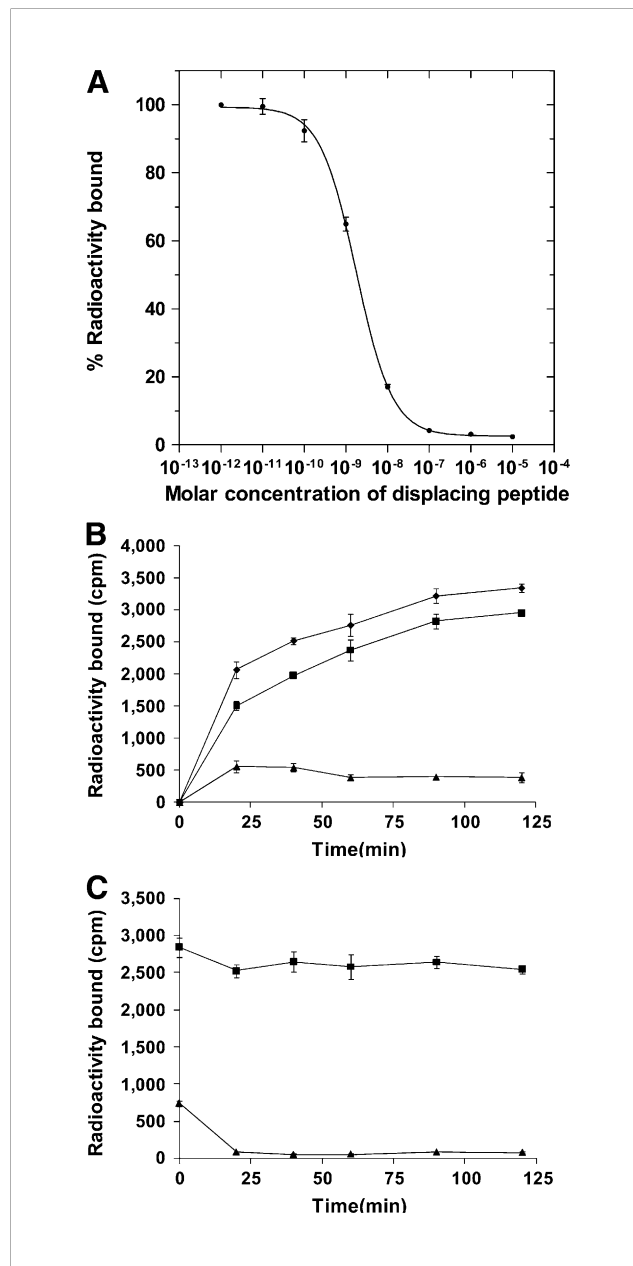 Both ^{111}In-labeled metal-cyclized and lactam bridge–cyclized α-MSH peptides exhibited greater melanoma uptake and lower renal uptake than ^{111}In-labeled disulfide bridge–cyclized α-MSH peptide (21,29). We have reported a novel class of melanoma-specific ^{111}In-labeled lactam bridge–cyclized α-MSH peptides for both primary and metastatic melanoma imaging (21,22). ^{111}In-DOTA-GlyGlu-CycMSH (Fig. 1), with a 12-amino acid peptide

	Biodistribution at...				2-h NDP	2-h L-lysine
Tissue	0.5 h	2 h	4 h	24 h	blockade	coinjection
%ID/g*						
Tumor	24.94 ± 4.58	19.39 ± 1.65	17.01 ± 2.54	10.53 ± 1.11	0.81 ± 0.03†	14.48 ± 3.25
Brain	0.21 ± 0.07	0.02 ± 0.01	0.06 ± 0.03	0.03 ± 0.01	0.01 ± 0.01	0.04 ± 0.01
Blood	3.33 ± 0.35	0.11 ± 0.07	0.05 ± 0.02	0.02 ± 0.01	0.07 ± 0.05	0.92 ± 0.48
Heart	1.24 ± 0.15	0.16 ± 0.10	0.12 ± 0.03	0.07 ± 0.05	0.06 ± 0.02	0.37 ± 0.02
Lung	2.45 ± 0.83	0.32 ± 0.10	0.10 ± 0.05	0.10 ± 0.03	0.30 ± 0.06	0.75 ± 0.21
Liver	2.75 ± 0.26	1.46 ± 0.20	1.72 ± 0.07	1.89 ± 0.14	1.46 ± 0.08	1.42 ± 0.30
Spleen	1.09 ± 0.33	0.41 ± 0.13	0.47 ± 0.13	0.32 ± 0.08	0.44 ± 0.02	0.43 ± 0.07
Stomach	3.20 ± 0.98	1.25 ± 0.24	1.49 ± 0.12	1.34 ± 0.42	0.36 ± 0.14	1.64 ± 0.78
Kidneys	16.20 ± 4.32	9.52 ± 0.44	9.99 ± 1.39	9.31 ± 0.91	11.56 ± 0.56	6.66 ± 0.62†
Muscle	0.60 ± 0.22	0.15 ± 0.08	0.10 ± 0.08	0.03 ± 0.01	0.02 ± 0.01	0.10 ± 0.08
Pancreas	1.18 ± 0.38	0.14 ± 0.02	0.16 ± 0.02	0.23 ± 0.08	0.12 ± 0.02	0.21 ± 0.05
Bone	1.34 ± 0.40	0.18 ± 0.10	0.22 ± 0.15	0.16 ± 0.03	0.05 ± 0.04	0.55 ± 0.14
Skin	4.11 ± 0.72	0.66 ± 0.23	0.53 ± 0.05	0.64 ± 0.16	0.29 ± 0.02	1.02 ± 0.09
%ID*						
Intestines	2.16 ± 0.28	1.40 ± 0.56	3.03 ± 1.06	1.41 ± 0.86	1.14 ± 0.47	1.85 ± 0.73
Urine	57.00 ± 3.91	82.23 ± 5.83	84.61 ± 5.21	87.29 ± 3.60	92.25 ± 1.56	76.79 ± 5.35
Tumor–to–normal-tissue uptake ratio						
Tumor-to-blood	7.49	176.27	340.20	526.50	11.57	15.74
Tumor-to-kidneys	1.54	2.04	1.70	1.13	0.07	2.17
Tumor-to-lung	10.18	60.59	170.10	105.30	2.70	19.31
Tumor-to-liver	9.07	13.28	9.89	5.57	0.55	10.20
Tumor-to-muscle	41.57	129.27	170.10	351.00	40.50	144.80
Tumor-to-skin	6.07	29.38	32.09	16.45	2.79	14.20

*Mean ± SD ($n = 5$).

†$P < 0.05$, significance comparison between tumor uptake of ^{111}In-DOTA-Nle-CycMSH$_{hex}$ with or without NDP-MSH blockade and kidney uptake of ^{111}In-DOTA-Nle-CycMSH$_{hex}$ with or without L-lysine coinjection.

Data are presented as percent %ID/g or as %ID (mean ± SD, $n = 5$).

ring, exhibited great potential as a melanoma-specific imaging probe in detecting both primary and metastatic melanoma lesions (21,22). However, tumor uptake of ^{111}In-DOTA-GlyGlu-CycMSH was 60.15% that of [111]In-
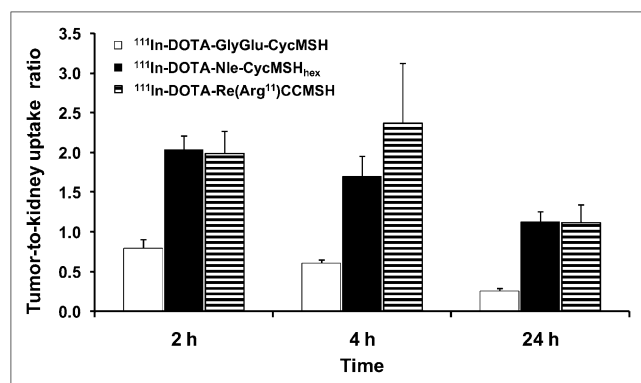

FIGURE 4. Tumor-to-kidney uptake ratios of ^{111}In-DOTA-GlyGlu-CycMSH, ^{111}In-DOTA-Nle-CycMSH$_{hex}$, and ^{111}In-DOTA-Re(Arg[11])CCMSH at 2, 4, and 24 h after injection. Calculated tumor-to-kidney uptake ratios of ^{111}In-DOTA-GlyGlu-CycMSH and ^{111}In-DOTA-Re(Arg[11])CCMSH were based on results published by Cheng et al. (17) and Miao et al. (21).

DOTA-Re(Arg[11])CCMSH, whereas kidney uptake of ^{111}In-DOTA-GlyGlu-CycMSH was 1.5 times renal uptake of ^{111}In-DOTA-Re(Arg[11])CCMSH at 2 h after injection in B16/F1 melanoma–bearing C57 mice (17,21). The structural differences between ^{111}In-DOTA-GlyGlu-CycMSH and ^{111}In-DOTA-Re(Arg[11])CCMSH (Fig. 1) indicated that the smaller size of the peptide ring might contribute to the more favorable melanoma targeting and pharmacokinetic properties of ^{111}In-DOTA-Re(Arg[11])CCMSH because there was an 8-amino acid peptide ring in ^{111}In-DOTA-Re(Arg[11])CCMSH, whereas there was a 12-amino acid peptide ring in ^{111}In-DOTA-GlyGlu-CycMSH. Moreover, it was reported that the lactam bridge–cyclized α-MSH peptide with a 6-amino acid peptide ring (Ac-Nle-c[Asp-His-D-Phe-Arg-Trp-Lys(CONH$_2$)]) displayed not only higher MC1 receptor–binding affinity but also a slower MC1 receptor dissociation rate than the native α-MSH peptide (27). Therefore, we synthesized a novel DOTA-conjugated lactam bridge–cyclized peptide with a 6-amino acid peptide ring (DOTA-Nle-CycMSH$_{hex}$) to examine the profound effect of the peptide ring size on the tumor and kidney uptake in this study.

The conjugation of DOTA to the N terminus of the peptide and the reduction of the peptide ring size did not
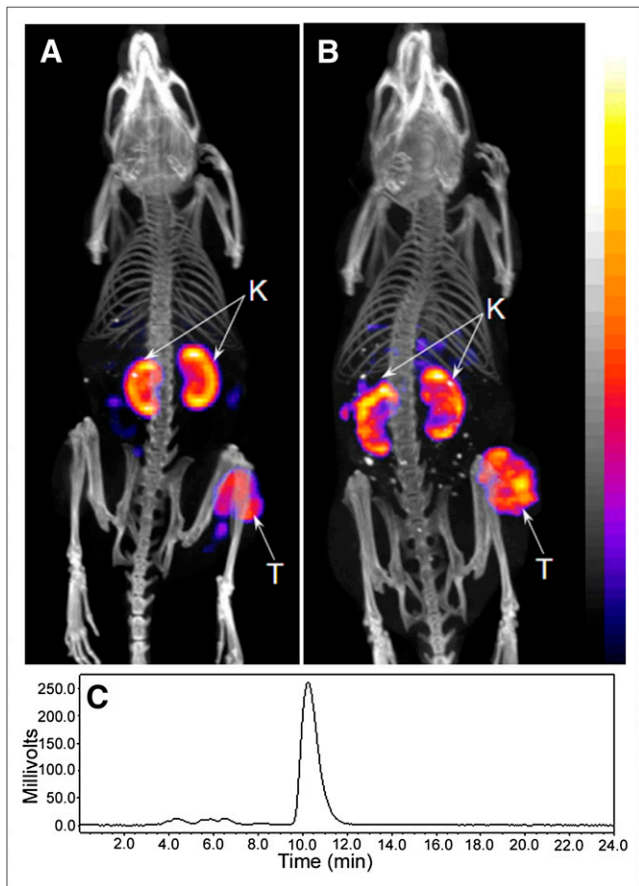
FIGURE 5. Whole-body SPECT/CT images of B16/F1 flank melanoma–bearing C57 mice at 2 (A) and 24 h (B) after injection of 37 MBq (1 mCi) of ^{111}In-DOTA-Nle-CycMSH$_{hex}$. Tumor (T) and kidneys (K) are highlighted with arrows on images. HPLC profile (C) of radioactive urine sample of B16/F1 melanoma–bearing C57 mouse at 2 h after injection of ^{111}In-DOTA-Nle-CycMSH$_{hex}$. ^{111}In-DOTA-Nle-CycMSH$_{hex}$ remained intact in urine at 2 h after injection.

sacrifice the MC1 receptor–binding affinity of DOTA-Nle-CycMSH$_{hex}$. DOTA-Nle-CycMSH$_{hex}$ exhibited 1.77 nM MC1 receptor–binding affinity in B16/F1 melanoma cells (Fig. 3A), whereas DOTA-GlyGlu-CycMSH and DOTA-Re(Arg^{11})CCMSH displayed 0.90 and 2.10 nM MC1 receptor–binding affinities in B16/F1 cells (17,21). ^{111}In-DOTA-Nle-CycMSH$_{hex}$ displayed rapid internalization and prolonged retention in B16/F1 melanoma cells, highlighting its potential as an effective imaging probe for melanoma detection and a therapeutic agent for melanoma treatment when labeled with a therapeutic radionuclide. As we anticipated, the strategy of reducing the ring size of the lactam bridge–cyclized α-MSH peptide resulted in improved tumor uptake and prolonged tumor retention. Compared with ^{111}In-DOTA-GlyGlu-CycMSH with a 12-amino acid peptide ring, ^{111}In-DOTA-Nle-CycMSH$_{hex}$ (Fig. 1) had only a 6-amino acid peptide ring. The tumor uptake (19.39 $\pm$ 2.72 %ID/g) of ^{111}In-DOTA-Nle-Cy-cMSH$_{hex}$ was 1.86 times that of ^{111}In-DOTA-GlyGlu-

CycMSH at 2 h after injection in B16/F1 melanoma–bearing C57 mice. ^{111}In-DOTA-Nle-CycMSH$_{hex}$ also exhibited more prolonged tumor retention than ^{111}In-DOTA-GlyGlu-CycMSH. At 24 h after injection, 54.3% of the ^{111}In-DOTA-Nle-CycMSH$_{hex}$ activity present at 2 h after injection (10.53 $\pm$ 1.11 %ID/g) remained in the tumors (Table 1), whereas only 22.8% of the ^{111}In-DOTA-GlyGlu-CycMSH radioactivity present at 2 h after injection (2.37 $\pm$ 0.28 %ID/g) remained in the tumors. Urinary analysis demonstrated that the ^{111}In-DOTA-Nle-CycMSH$_{hex}$ remained intact 2 h after injection (Fig. 5C). It is likely that both high in vivo stability of ^{111}In-DOTA-Nle-CycMSH$_{hex}$ and low MC1 receptor dissociation rate (27) contributed to the rapid high melanoma uptake (24.94 $\pm$ 4.58 %ID/g at 0.5 h after injection) and prolonged tumor retention (10.53 $\pm$ 1.11 %ID/g at 24 h after injection) of ^{111}In-DOTA-Nle-CycMSH$_{hex}$ in B16/F1 melanoma–bearing C57 mice.

The reduction of the peptide ring size also decreased the nonspecific kidney uptake of ^{111}In-DOTA-Nle-CycMSH$_{hex}$, compared with ^{111}In-DOTA-GlyGlu-CycMSH (21), at 2 and 4 h after injection. Renal uptake of ^{111}In-DOTA-Nle-CycMSH$_{hex}$ was only 72.8% and 82.4% that of ^{111}In-DOTA-GlyGlu-CycMSH at 2 and 4 h after injection, respectively. Renal uptake of ^{111}In-DOTA-Nle-CycMSH$_{hex}$ was further reduced with L-lysine coinjection by 30% at 2 h after injection, demonstrating that the electrostatic interaction between ^{111}In-DOTA-Nle-CycMSH$_{hex}$ and kidney cells played an important role in renal uptake of ^{111}In-DOTA-Nle-CycMSH$_{hex}$. The synergistic effects of an increase in tumor uptake and a decrease in renal uptake dramatically improved the tumor-to-kidney uptake ratios of ^{111}In-DOTA-Nle-CycMSH$_{hex}$ at all time points investigated in this study. Improved tumor uptake and decreased kidney uptake resulted in tumor-to-kidney uptake ratios of ^{111}In-DOTA-Nle-CycMSH$_{hex}$ that were superior to those of ^{111}In-DOTA-GlyGlu-CycMSH at 2, 4, and 24 h after injection. The tumor-to-kidney uptake ratios of ^{111}In-DOTA-Nle-CycMSH$_{hex}$ were 2.55, 2.79, and 4.35 times those of ^{111}In-DOTA-GlyGlu-CycMSH at 2, 4, and 24 h after injection, respectively (Fig. 4). ^{111}In-DOTA-Nle-CycMSH$_{hex}$ remained intact in the urine (Fig. 5C), whereas all ^{111}In-DOTA-GlyGlu-CycMSH transformed into 2 polar metabolites in the urine at 2 h after injection (21), possibly contributing to the decreased renal uptake of ^{111}In-DOTA-Nle-CycMSH$_{hex}$.

Recently, ^{99m}Tc-labeled lactam bridge–cyclized α-MSH peptides ([Ac-Nle^4,Asp^5,D-Phe^7,Lys^{11}(pz-^{99m}Tc(CO)$_3$)]α-MSH$_{4-11}$ and ^{99m}Tc(CO)$_3$-pz-βAla-Nle-cyclo[Asp-His-D-Phe-Arg-Trp-Lys]-NH$_2$) have been reported for melanoma targeting (30,31). ^{99m}Tc(CO)$_3$-pz-βAla-Nle-cyclo[Asp-His-D-Phe-Arg-Trp-Lys]-NH$_2$ exhibited melanoma uptake (11.31 $\pm$ 1.81 %ID/g) superior to that of [Ac-Nle^4,Asp^5, D-Phe^7,Lys^{11}(pz-^{99m}Tc(CO)$_3$)]α-MSH$_{4-11}$ (4.24 $\pm$ 0.94 %ID/g) at 4 h after injection in B16/F1 melanoma–bearing C57 mice. However, ^{99m}Tc(CO)$_3$-pz-βAla-Nle-cyclo[Asp-His-D-Phe-Arg-Trp-Lys]-NH$_2$ displayed high accumulation

and prolonged retention in both liver (22.86 ± 1.17 %ID/g) and kidneys (32.12 ± 1.57 %ID/g) at 4 h after injection, possibly limiting its potential application in metastatic melanoma imaging. In this study, tumor uptake of ^{111}In-DOTA-Nle-CycMSH$_{hex}$ was 1.5 times that of ^{99m}Tc(CO)$_3$-pz-βAla-Nle-cyclo[Asp-His-D-Phe-Arg-Trp-Lys]-NH$_2$ at 4 h after injection, whereas liver and kidney uptake of ^{111}In-DOTA-Nle-CycMSH$_{hex}$ were only 7.5% and 31.1% that of ^{99m}Tc(CO)$_3$-pz-βAla-Nle-cyclo[Asp-His-D-Phe-Arg-Trp-Lys]-NH$_2$ at 4 h after injection. The dramatic increase in tumor uptake and decrease in liver and kidney uptake of ^{111}In-DOTA-Nle-CycMSH$_{hex}$ were likely due to the structural differences between ^{99m}Tc(CO)$_3$-pz-βAla-Nle-cyclo[Asp-His-D-Phe-Arg-Trp-Lys]-NH$_2$ and ^{111}In-DOTA-Nle-CycMSH$_{hex}$.

Currently, metal-cyclized ^{111}In-DOTA-Re(Arg^{11})CCMSH showed the highest melanoma uptake among all reported ^{111}In-labeled linear and cyclic α-MSH peptides (*17*). The tumor uptake of ^{111}In-DOTA-Re(Arg^{11})CCMSH was 17.29 ± 2.49 %ID/g, 17.41 ± 5.63 %ID/g, and 8.19 ± 1.63 %ID/g at 2, 4, and 24 h after injection, respectively (*17*). Remarkably, ^{111}In-DOTA-Nle-CycMSH$_{hex}$ exhibited 1.12, 0.98, and 1.29 times the tumor uptake of ^{111}In-DOTA-Re(Arg^{11})CCMSH at 2, 4, and 24 h after injection, respectively. Meanwhile, ^{111}In-DOTA-Nle-CycMSH$_{hex}$ showed renal uptake that was slightly higher than but similar to ^{111}In-DOTA-Re(Arg^{11})CCMSH at 2 and 4 h after injection. ^{111}In-DOTA-Nle-CycMSH$_{hex}$ exhibited tumor-to-kidney ratios comparable to ^{111}In-DOTA-Re(Arg^{11})CCMSH at 2 and 24 h after injection despite the fact that the tumor-to-kidney uptake ratio of ^{111}In-DOTA-Nle-CycMSH$_{hex}$ was 28% less than that of ^{111}In-DOTA-Re(Arg^{11})CCMSH at 4 h after injection. It was reported that a single-dose treatment of 7.4 MBq (200 µCi) of ^{212}Pb-labeled DOTA-Re(Arg^{11})CCMSH resulted in 44% cures in B16/F1 melanoma–bearing mice (*11*). Accordingly, it would be likely that treatment with ^{212}Pb-labeled DOTA-Nle-CycMSH$_{hex}$ would yield similar quantitative therapeutic effect for melanoma in the future because ^{111}In-DOTA-Nle-CycMSH$_{hex}$ displayed tumor-to-kidney ratios comparable to ^{111}In-DOTA-Re(Arg^{11})CCMSH at 2 and 24 h after injection.

CONCLUSION

The ring size of the ^{111}In-labeled lactam bridge–cyclized α-MSH peptide exhibited a profound effect on its melanoma-targeting and pharmacokinetic properties. The reduction of the peptide ring size dramatically increased the melanoma uptake and decreased the renal uptake of ^{111}In-DOTA-Nle-CycMSH$_{hex}$, providing a new insight into the design of novel radiolabeled lactam bridge–cyclized α-MSH peptide for melanoma imaging and treatment.

ACKNOWLEDGMENTS

REFERENCES

1. Jemal A, Siegel R, Ward E, Hao Y, Xu J, Thun MJ. Cancer statistics, 2009. *CA Cancer J Clin.* 2009;59:225–249.
2. Alonso O, Martinez M, Delgado L, et al. Staging of regional lymph nodes in melanoma patients by means of ^{99m}Tc-MIBI scintigraphy. *J Nucl Med.* 2003;44:1561–1565.
3. Nabi HA, Zubeldia JM. Clinical application of ^{18}F-FDG in oncology. *J Nucl Med Technol.* 2002;30:3–9.
4. Dimitrakopoulou-Strauss A, Strauss LG, Burger C. Quantitative PET studies in pretreated melanoma patients: a comparison of 6-[^{18}F]fluoro-L-DOPA with ^{18}F-FDG and ^{15}O-water using compartment and non-compartment analysis. *J Nucl Med.* 2001;42:248–256.
5. Miao Y, Whitener D, Feng W, Owen NK, Chen J, Quinn TP. Evaluation of the human melanoma targeting properties of radiolabeled α-melanocyte stimulating hormone peptide analogues. *Bioconjug Chem.* 2003;14:1177–1184.
6. Miao Y, Owen NK, Whitener D, Gallazzi F, Hoffman TJ, Quinn TP. In vivo evaluation of ^{188}Re-labeled α-melanocyte stimulating hormone peptide analogs for melanoma therapy. *Int J Cancer.* 2002;101:480–487.
7. Chen J, Cheng Z, Hoffman TJ, Jurisson SS, Quinn TP. Melanoma-targeting properties of ^{99m}technetium-labeled cyclic α-melanocyte-stimulating hormone peptide analogues. *Cancer Res.* 2000;60:5649–5658.
8. Siegrist W, Solca F, Stutz S, et al. Characterization of receptors for α-melanocyte-stimulating hormone on human melanoma cells. *Cancer Res.* 1989;49:6352–6358.
9. Tatro JB, Reichlin S. Specific receptors for α-melanocyte-stimulating hormone are widely distributed in tissues of rodents. *Endocrinology.* 1987;121:1900–1907.
10. Miao Y, Owen NK, Fisher DR, Hoffman TJ, Quinn TP. Therapeutic efficacy of a ^{188}Re-labeled α-melanocyte-stimulating hormone peptide analog in murine and human melanoma-bearing mouse models. *J Nucl Med.* 2005;46:121–129.
11. Miao Y, Hylarides M, Fisher DR, et al. Melanoma therapy via peptide-targeted α-radiation. *Clin Cancer Res.* 2005;11:5616–5621.
12. Froidevaux S, Calame-Christe M, Tanner H, Eberle AN. Melanoma targeting with DOTA-α-melanocyte-stimulating hormone analogs: structural parameters affecting tumor uptake and kidney uptake. *J Nucl Med.* 2005;46:887–895.
13. Froidevaux S, Calame-Christe M, Schuhmacher J, et al. A gallium-labeled DOTA-α-melanocyte-stimulating hormone analog for PET imaging of melanoma metastases. *J Nucl Med.* 2004;45:116–123.
14. Froidevaux S, Calame-Christe M, Tanner H, Sumanovski L, Eberle AN. A novel DOTA-α-melanocyte-stimulating hormone analog for metastatic melanoma diagnosis. *J Nucl Med.* 2002;43:1699–1706.
15. Wei L, Butcher C, Miao Y, et al. Synthesis and biologic evaluation of ^{64}Cu-labeled rhenium-cyclized α-MSH peptide analog using a cross-bridged cyclam chelator. *J Nucl Med.* 2007;48:64–72.
16. Miao Y, Benwell K, Quinn TP. ^{99m}Tc- and ^{111}In-labeled α-melanocyte-stimulating hormone peptides as imaging probes for primary and pulmonary metastatic melanoma detection. *J Nucl Med.* 2007;48:73–80.
17. Cheng Z, Chen J, Miao Y, Owen NK, Quinn TP, Jurisson SS. Modification of the structure of a metallopeptide: synthesis and biological evaluation of ^{111}In-labeled DOTA-conjugated rhenium-cyclized α-MSH analogues. *J Med Chem.* 2002;45:3048–3056.
18. Cheng Z, Xiong Z, Subbarayan M, Chen X, Gambhir SS. ^{64}Cu-labeled α-melanocyte-stimulating hormone analog for MicroPET imaging of melanocortin 1 receptor expression. *Bioconjug Chem.* 2007;18:765–772.
19. Wei L, Miao Y, Gallazzi F, et al. Ga-68 labeled DOTA-rhenium cyclized α-MSH analog for imaging of malignant melanoma. *Nucl Med Biol.* 2007;34:945–953.
20. Cantorias MV, Figueroa SD, Quinn TP, et al. Development of high-specific-activity ^{68}Ga-labeled DOTA-rhenium-cyclized α-MSH peptide analog to target MC1 receptors overexpressed by melanoma tumors. *Nucl Med Biol.* 2009;36:505–513.

21. Miao Y, Gallazzi F, Guo H, Quinn TP. ^{111}In-labeled lactam bridge-cyclized α-melanocyte stimulating hormone peptide analogues for melanoma imaging. *Bioconjug Chem.* 2008;19:539–547.

22. Guo H, Shenoy N, Gershman BM, Yang J, Sklar LA, Miao Y. Metastatic melanoma imaging with an ^{111}In-labeled lactam bridge-cyclized α-melanocyte-stimulating hormone peptide. *Nucl Med Biol.* 2009;36:267–276.

23. Sawyer TK, Hruby VJ, Darman PS, Hadley ME. [half-Cys[4],half-Cys[10]]-α-melanocyte-stimulating hormone: a cyclic α-melanotropin exhibiting super-agonist biological activity. *Proc Natl Acad Sci USA.* 1982;79:1751–1755.

24. Al-Obeidi F, Hadley ME, Pettitt BM, Hruby VJ. Design of a new class of superpotent cyclic α-melanotropins based on quenched dynamic simulations. *J Am Chem Soc.* 1989;111:3413–3416.

25. Al-Obeidi F. de L Castrucci AM, Hadley ME, Hruby VJ. Potent and prolonged-acting cyclic lactam analogs of α-melanotropin: design based on molecular dynamics. *J Med Chem.* 1989;32:2555–2561.

26. Fung S, Hruby VJ. Design of cyclic and other templates for potent and selective peptide α-MSH analogues. *Curr Opin Chem Biol.* 2005;9:352–358.

27. Haskell-Luevano C, Miwa H, Dickinson C, et al. Characterizations of the unusual dissociation properties of melanotropin peptides from the melanocortin receptor, hMC1R. *J Med Chem.* 1996;39:432–435.

28. Haskell-Luevano C, Toth K, Boteju L, et al. β-Methylation of the Phe[7] and Trp[9] melanotropin side chain pharmacophores affects ligand-receptor interactions and prolonged biological activity. *J Med Chem.* 1997;40:2740–2749.

29. Chen J, Cheng Z, Owen NK, et al. Evaluation of an ^{111}In-DOTA-rhenium cyclized α-MSH analog: a novel cyclic-peptide analog with improved tumor-targeting properties. *J Nucl Med.* 2001;42:1847–1855.

30. Raposinho PD, Xavier C, Correia JD, Falcao S, Gomes P, Santos I. Melanoma targeting with α-melanocyte stimulating hormone analogs labeled with fac-[[99m]Tc(CO)$_3$][+]: effect of cyclization on tumor-seeking properties. *J Biol Inorg Chem.* 2008;13:449–459.

31. Raposinho PD, Correia JD, Alves S, Botelho MF, Santos AC, Santos I. A [99m]Tc(CO)$_3$-labeled pyrazolyl–α-melanocyte-stimulating hormone analog conjugate for melanoma targeting. *Nucl Med Biol.* 2008;35:91–99.